Self-assembly of rod-coil-rod triblock copolymers: A route toward hierarchical liquid crystalline structures

CrossMark

Yongliang Li [a], Tao Jiang [b], Liquan Wang [a, **], Shaoliang Lin [a], Jiaping Lin [a, *]

[a] Shanghai Key Laboratory of Advanced Polymeric Materials, State Key Laboratory of Bioreactor Engineering, Key Laboratory for Ultrafine Materials of Ministry of Education, School of Materials Science and Engineering, East China University of Science and Technology, Shanghai 200237, China
[b] Beijing Institute of Nanoenergy and Nanosystems, Chinese Academy of Sciences, National Center for Nanoscience and Technology (NCNST), Beijing 100083, China

ABSTRACT

Brownian dynamics simulations are performed to investigate self-assembly behavior of rod-coil-rod triblock copolymers that contain two types of rod blocks. These rod-coil-rod triblock copolymers are capable of self-assembling into liquid crystalline (LC) structures with hierarchy. The morphologies of the hierarchical LC structures can be controlled by temperature, symmetry of LC blocks, and block length. As the temperature decreases, a transition from isotropic lamellae to smectic C lamellae is observed, accompanied by an increase in orientational ordering and tilt angle of rod blocks. For the hierarchical lamellae-in-lamella structures formed by symmetric block copolymers, there are two LC phases with nearly identical ordering and tilt angle for two rod blocks. While for the lamellae-in-lamellae formed by asymmetric block copolymers, the two LC phases exhibit two different length scales with diverse ordering degrees and tilt angles. By adjusting the lengths of coil and rod blocks, the stability regions of the structures are mapped out in space of the block length versus the temperature. The findings in the present work could provide useful information for understanding the self-assembly behavior of rod-coil-rod triblock copolymers and designing hierarchical liquid crystalline structures.

© 2016 Elsevier Ltd. All rights reserved.

1. Introduction

Rod-coil block copolymers have a capability to self-assemble into various microstructures with liquid crystalline (LC) phases, including rectangular column, oblique column, and tetragon, *etc.* [1–4] In these LC structures, the combination of ordered packing of rod blocks and separation of immiscible rod/coil blocks determines the structural characteristics [5–7]. Generally, the LC microstructures possess only one structure period at the nanoscale, for example, the smectic structure formed by rod-coil diblock copolymers. When introducing two kinds of chemically different LC molecules or one kind of LC molecules with various block lengths into the system, hierarchical LC structures with double periodicities can be obtained, showing multiscale spatial orders over both LC and amorphous domains [8]. Such hierarchical LC structures can find important applications in fields such as optoelectronic devices,

high-modulus fibers, and biosystems [9–11].

Recently, hierarchical microstructures with multiple periods at different length scales have attracted great interests, which focus on the design of various hierarchical structures by tuning molecular topologies and chain compositions [12–24]. These structures are mainly prepared by the self-assembly of flexible copolymers. In contrast, the experimental studies on the hierarchical LC structures are very limited [20–24]. The copolymers consisting of two kinds of rod blocks are one candidate for self-assembling into hierarchical LC structures. Iatrou et al. synthesized poly(γ-benzyl-ʟ-glutamate)-*b*-poly(ʟ-proline) (PBLG-*b*-PLP) polypeptides in which both the PBLG and PLP adopt rigid helical conformations [20]. It was found that these rod-rod copolypeptides can form hierarchical LC fibers with the PBLG preferentially oriented along the fiber axis and the PLP helices unoriented. They also reported the rod-rod diblock copolymers composed of poly(benzyl-ʟ-hydroxyproline) (PBLHyP) and PBLG are able to form hierarchical LC structures such as zig-zag lamellar structures, due to the mismatch in the packing periodicities of the dissimilar PBLG and PBLHyP helices [21]. Haataja et al. investigated the self-assembly behavior of poly(γ-benzyl-ʟ-gluta-mate)-*block*-poly(ʟ-lysine) (PBLG-*b*-PLL) in which the PLL amino

* Corresponding author.
** Corresponding author.
 E-mail addresses: lq_wang@ecust.edu.cn (L. Wang), jlin@ecust.edu.cn (J. Lin).

residues were ionically complexed to di-*n*-butyl phosphate (diC4P) [22]. These PBLG-*b*-PLL(diC4P) rod-rod systems were found to form double smectic-like structures with alternating PBLG and PLL(diC4P) smectic layers of approximately perpendicular alignment of both types of α-helices. These works indicate that the rod-rod block copolymers are promising in constructing hierarchical LC structures with various LC states in the domains. Since the rod-rod block copolymers such as PBLG-*b*-PLP and PBLG-*b*-PBLHyP can be regarded as the rod-rod copolymers with negligible coil midblocks, the rod-coil-rod copolymers can be the general architectures for hierarchical LC structures. Despite of their capability, the understanding on the self-assembly of rod-coil-rod copolymers into hierarchical LC structures is still limited and more detailed exploration is necessary.

Apart from the experimental investigations, theory and computer simulations have emerged as powerful tools to study the self-assembly behavior of block copolymers comprised of rod blocks [25—40]. They could provide more straightforward results than pure experiments and overcome the limitation inherent in experiments. So far, various approaches, such as self-consistent field theory (SCFT) [25—28], Brownian dynamics (BD) simulations [29—31], and dissipative particle dynamics (DPD) simulations [32,33], were successfully applied to investigate the phase behavior of the block copolymers with rod blocks. In our previous work, we revealed that **C**′(**RC**)$_n$**R**′ multiblock copolymers can self-assemble into a series of smectic-in-smectic, isotropic-in-smectic, and smectic-in-amorphous phases by using real-space SCFT [8]. The hierarchical LC structures exhibit not only double periodicities in overall structure but also double orientational orders of rod blocks. However, the architecture of the **C**′(**RC**)$_n$**R**′ copolymers is complex and it is difficult to be prepared in experiments. In contrast with the **C**′(**RC**)$_n$**R**′ copolymers, rod-coil-rod block copolymers could more easily be synthesized and therefore merit more attention. Currently, there are several investigations on the self-assembly of rod-coil-rod copolymers in dilute solutions and bulks by theoretical calculations and computer simulations [41—45]. Note that these studies are concentrated on the rod-coil-rod copolymers with identical kinds of two end rod blocks and hierarchical LC structures cannot be formed. Therefore, computer simulation study on the self-assembly of rod-coil-rod copolymers into hierarchical LC structures is still lacking. The BD simulations can be used to investigate the self-assembly of the rod-coil-rod copolymers due to their success in studying the phase behavior of the copolymers with rod blocks [29—31,46—48]. For example, Glotzer et al. performed BD simulations on rod-coil diblock copolymers, and obtained various LC phases, including cubic phase, smectic C phase, tetragonally perforated lamellar phase, and honeycomb phase [31]. The morphologies of LC structures were found to be dependent of rod aspect ratio, coil length, and temperature.

In this work, we performed a Brownian dynamics simulation to study the self-assembly behavior of rod-coil-rod triblock copolymers. The effects of temperature, symmetry of LC blocks, and length of blocks on the formed hierarchical LC structures were examined. The packing ordering and tilt angle were characterized and compared for two cases, *i.e.*, symmetric block copolymers and asymmetric block copolymers. By systemically changing the block length and the temperature, the stability regions of the structures were mapped out in the space of block length versus temperature.

2. Model and method

We considered a system of rod-coil-rod triblock copolymers with two types of rod blocks, and constructed a coarse-grained model, as typically shown in Fig. 1. The block copolymer is denoted as **R**$_n$**C**$_m$**R**′$_n$, where the subscripts represent the bead number on
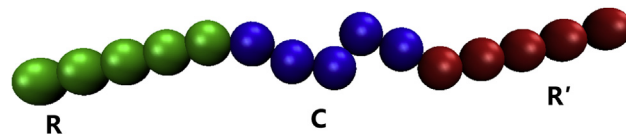
Fig. 1. Coarse-grained model of a rod-coil-rod triblock copolymer. The block copolymer is denoted by the type of **R**$_n$**C**$_m$**R**′$_n$. The beads colored by green, blue, and red represent rigid **R** block, flexible **C** block, and rigid **R**′ block, respectively. (For interpretation of the references to colour in this figure legend, the reader is referred to the web version of this article.)

each block. The **R** and **R**′ rod blocks were both modeled as *n* beads linked in a linear geometry [31,49]. Each rod block was treated as a rigid body without bonding potential between beads. The spacing between adjacent spheres for **R** and **R**′ blocks were defined as *d* and *d*′, which determines the degree of roughness within the rods. The lengths (in units of σ) of **R** and **R**′ blocks were given by $L = [(n-1)d+1]$ and $L' = [(n-1)d'+1]$, respectively. Therefore, $d = d'$ corresponds to a symmetric copolymer and $d \neq d'$ corresponds to an asymmetric copolymer. The coil block consists of *m* beads bonded together *via* a finite extensible nonlinear elastic (FENE) potential [50,51], given by

$$U_{\text{FENE}} = \begin{cases} -0.5kR_0^2 \ln\left[1 - \left(\dfrac{r}{R_0}\right)^2\right], & r \leq R_0 \\ \infty, & r > R_0 \end{cases} \tag{1}$$

where *k* is the bond spring constant, R_0 is the maximum extended length of bonds, and *r* is the distances between adjacent beads. In this work, we set *k* and R_0 to be 30ε/σ [2] (ε is the energy unit) and 1.5σ so as to ensure stiff bonds and avoid chain crossing [50]. The bonds between rod block and coil block also adopt the FENE potential.

The nonbonding potential U_{ij} is given by the standard Lennard-Jones 12:6 potential acting between any pair of *i*-th and *j*-th beads [41]:

$$U_{ij} = \begin{cases} 4\varepsilon_{ij}\left[\left(\dfrac{\sigma}{r_{ij}}\right)^{12} - \left(\dfrac{\sigma}{r_{ij}}\right)^{6} - \left(\dfrac{\sigma}{r_{ij}^{\text{c}}}\right)^{12} + \left(\dfrac{\sigma}{r_{ij}^{\text{c}}}\right)^{6}\right], & r_{ij} \leq r_{ij}^{\text{c}} \\ 0, & r_{ij} > r_{ij}^{\text{c}} \end{cases} \tag{2}$$

where r_{ij}^{c} is the cutoff distance, $r_{ij} = |\mathbf{r}_i - \mathbf{r}_j|$ with $\mathbf{r}_i$ and $\mathbf{r}_j$ being the position vectors of the *i*-th and *j*-th beads, and ε_{ij} is the interaction parameter between *i*-th and *j*-th beads. The compatibility of polymer blocks in this model is realized by introducing different cutoff distances of LJ potential [52,53]. The distances r_{CC}^{c}, r_{RC}^{c}, $r_{\text{R}'\text{C}}^{\text{c}}$ and $r_{\text{RR}'}^{\text{c}}$ were all set as $2^{1/6}$ to realize the repulsive **C**-**C**, **R**-**C**, **R**′-**C** and **R**-**R**′ interactions, while the cutoff distances r_{RR}^{c} and $r_{\text{R}'\text{R}'}^{\text{c}}$ were chosen as 2.5 to indicate that the **R**-**R** and **R**′-**R**′ interactions are attractive. These selections of r_{ij}^{c} imply that the **R** and **R**′ blocks are hydrophobic and the **C** blocks are hydrophilic. The diameter σ of LJ bead is kept at unity for any pair of species, and the interaction parameters ε_{ij} between any pair of species are also unity.

All the simulations were performed in a cubic cell with periodic boundary conditions using a Brownian dynamics algorithm with the temperature controlling method (NVT ensemble) [54]. The beads are coupled to a heat bath, and the equations of motion are written by

$$m_i \frac{d^2\mathbf{r}_i}{dt^2} = \mathbf{F}_i - \Gamma_0 \frac{d\mathbf{r}_i}{dt} + \mathbf{W}_i(t) \tag{3}$$

where m_i is the mass of the i-th bead, Γ_0 is the friction constant, and $\mathbf{F}_i$ is the force acting on the i-th bead calculated by the potential energies consisting of U_{FENE} and U_{ij}. In the Brownian dynamics, the effect of solvent molecules is implicitly treated by a noise term $\mathbf{W}_i(t)$, which can be calculated through the fluctuation-dissipation relation [55]:

$$\langle \mathbf{W}_i(t) \cdot \mathbf{W}_j(t') \rangle = 6k_B T \Gamma_0 \delta_{ij} \delta(t - t') \tag{4}$$

The equations of motion were solved by the leapfrog integration algorithm using a time step of $\Delta t = 0.006\tau$ (τ is the time unit). Note that the rotational freedom degrees of rod blocks were incorporated using the equations for rotation of linear bodies [56]. We started the simulations from a random structure, and then equilibrated the copolymer systems athermally (repulsive interactions only) at a high temperature ($T = 6.0$). Subsequently, the systems were cooled to the target temperature by decrementing the temperature at $\Delta T = 0.1$. Note that the present work are mainly focused on the annealing cases and found that the cooling/heating rates show negligible influence on the results. If the rate is very high, there would be some hystereses or metastable states, but it is beyond the present consideration. Finally, the simulations run 5×10^7 time steps until the temperature reaches 1.0. The reduced temperature T can be converted into the real unit through the relation of $1T = \varepsilon/R = 60.1$ K, where the energy unit ε is chosen as 0.5 kJ/mol, and R is the gas constant [46]. Therefore, as the reduced temperature changes from 6.0 to 1.0, the actual temperature decreases from 360.6 K to 60.1 K.

Here we defined the volume fraction φ of triblock copolymers, given by $N_{chain}[(n-1)(d + d')\,\pi\sigma^2/4 + (m+2)\pi\sigma^3/6]/V$ for rod blocks containing overlapped spheres and $N_{bead}\pi\sigma^3/6V$ for rod blocks without overlapped spheres, where V is the box volume, and N_{chain} and N_{bead} are the total numbers of polymer chains and beads, respectively. To simulate a neat system (without solvents), we need to set a high volume fraction such as $\varphi = 0.45$ [30]. By assigning the molecule structure, volume fraction, and chain number, the volume of simulation box can be calculated. To avoid the effect of finite system size, the systems of $N_{chain} = 500$, 1000, and 2000 were respectively considered for the $\mathbf{R}_5\mathbf{C}_4\mathbf{R}'_5$ copolymers ($d = d' = \sigma$) at $\varphi = 0.45$ and similar results were obtained. In the following simulations, $n = 5$, $d = \sigma$, and $\varphi = 0.45$ were fixed, while the values of d' and m were variable to model various lengths of rod and coil blocks. All BD runs were carried out by using the large scale atomic/molecular massively parallel simulator (LAMMPS) which was developed by Sandia National Laboratories [57].

In addition, the orientation degree of rod blocks in the hierarchical LC structures can be characterized by order parameter S. The S_i for i-th rod block is defined by:

$$S_i = \frac{3(\mathbf{u}_i \cdot \mathbf{u}_d)^2 - 1}{2} \tag{5}$$

where $\mathbf{u}_i$ is the normalized vector of i-th rod block, $\mathbf{u}_d$ is the normalized vector of orientation direction, which is determined by iteration to find the maximum value of S by dividing the polar-coordinate space into pieces. The order parameter S of rod blocks within a specific structure is the average value of S_i. We also calculated the tilt angle θ of rod blocks with respect to the interfacial normal in formed smectic C structures at a low temperature. The tilt angle ($<90°$) was captured for both $\mathbf{R}$ and $\mathbf{R}'$ blocks, which satisfies the following relation

$$\cos(\theta) = |\mathbf{u}_d \cdot \mathbf{u}_l| \tag{6}$$

where $\mathbf{u}_l$ is the normalized vector perpendicular to the interface of the lamellae.

3. Results and discussion

In this work, self-assembly of rod-coil-rod triblock copolymers in bulk was studied and the effects of temperature and molecular architecture were examined. The simulations were performed for two cases, *i.e.*, symmetric block copolymers and asymmetric block copolymers. For the symmetric block copolymers, we chose the $\mathbf{R}_5\mathbf{C}_m\mathbf{R}'_5$ model with $d = d'$ (0.5–1.0σ), and therefore the lengths of the $\mathbf{R}$ and $\mathbf{R}'$ blocks are the same (3.0–5.0σ). The length of coil blocks was denoted by the coil bead number m varying from 2 to 5. On studying the effect of the length of coil blocks, the lengths of $\mathbf{R}$ and $\mathbf{R}'$ blocks were both kept as 5.0σ. While for investigating the influence of the length of rod blocks, the m was set to be 4. For the asymmetric block copolymers, the d was fixed as σ, but the d' was changed from 0.5σ to σ corresponding to the $\mathbf{R}'$ block lengths of 3.0–5.0σ. We adjusted the length of $\mathbf{R}'$ blocks by changing the adjacent space d' between beads instead of the bead number to ensure the same density for each system. The length of coil blocks was also varied between 2 and 5. The chain number of block copolymers was set to be 1000 for both cases.

3.1. LC structures self-assembled from symmetric triblock copolymers

It is well-known that the packing ordering of thermotropic liquid crystal polymers is very sensitive to the temperature [32,33]. In high-temperature region, the LC molecules hold an isotropic state, while they can exhibit ordered packing in low-temperature region. By cooling the symmetric $\mathbf{R}_5\mathbf{C}_m\mathbf{R}'_5$ copolymer systems from $T = 6.0$ to $T = 1.0$, the morphology transformation of LC structures, as well as the ordering degree and tilt angle of the rod blocks were studied. In addition, we compared the order parameter of rod blocks of the triblock copolymers with that of rod-coil diblock copolymers. Then the effects of the lengths of the coil blocks and the rod blocks on the LC structures and chain packing were examined.

Fig. 2a–c presents the temperature dependence of LC structures formed by $\mathbf{R}_5\mathbf{C}_4\mathbf{R}'_5$ triblock copolymers with $L = L' = 5.0\sigma$. At a high temperature ($T = 5.5$), an isotropic structure with the blocks randomly packed was initially obtained (Fig. 2a). When the temperature is 3.5, the isotropic structure was found to transform into a lamellar structure with low ordering of rod blocks. As the temperature decreases, the rod blocks tend to pack in a parallel fashion, and a more ordered lamella was formed at $T = 2.5$ (Fig. 2c). With further decreasing the temperature to 1.0, the copolymers self-assemble into a highly ordered smectic C lamellar structure, as shown in Fig. 2d. In the smectic C lamellae, both the $\mathbf{R}$ and $\mathbf{R}'$ blocks take the orientation of smectic C, that is, a tilt angle exists between the orientational direction and the lamellar normal direction. Further decreasing the temperature, the crystalline structure was finally observed.

To characterize the variation of the ordering of rod blocks in the structural evolution of $\mathbf{R}_5\mathbf{C}_4\mathbf{R}'_5$ triblock copolymers, we calculated the order parameters for two rod blocks, which are shown in Fig. 2e. As shown in the figure, the variation of order parameters S as a function of the temperature exhibits the same tendency for the $\mathbf{R}$ and $\mathbf{R}'$ blocks. When the temperature is higher than 3.7, the S is close to zero, indicating that the rod blocks are in disordered state (Dis). In the region of $2.9 < T < 3.7$, the S is still lower although a
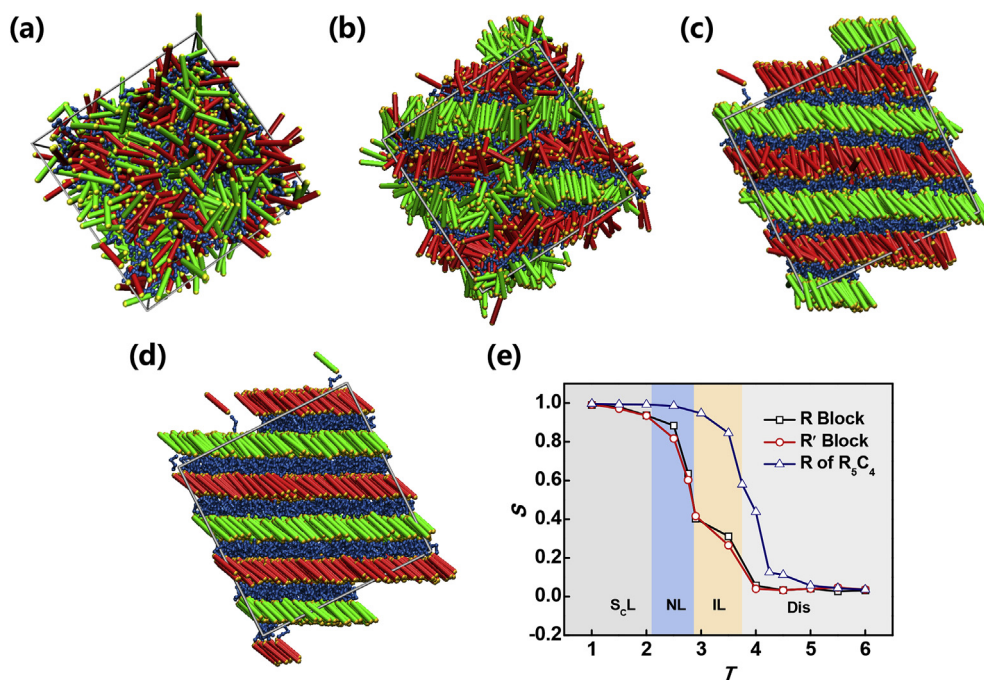
Fig. 2. Morphologies of LC structures formed by symmetric $R_5C_4R'_5$ triblock copolymers with $L = L' = 5.0\sigma$ at various temperatures: (a) $T = 5.5$, (b) $T = 3.5$, (c) $T = 2.5$, and (d) $T = 1.0$. (e) Order parameters S for the **R** and **R'** blocks as functions of the temperature. Regions of disordered phase (Dis), isotropic lamella (IL), nematic lamella (NL), and smectic C lamella (S_CL) are marked. The order parameter for **R** block of R_5C_4 diblock copolymers was also shown for comparison.

lamella structure is formed (Fig. 2b). We referred to this kind of lamellar structure with $S < 0.43$ as an isotropic lamella (IL). In the region of $2.1 < T < 2.9$, the order parameters increase gradually with the temperature. To distinguish the IL, the lamella with $0.43 < S < 0.9$ was defined as a nematic lamella (NL). When the temperature is below 2.1, the order parameter is higher than 0.9, where the lamella with high ordering is named as a smectic C lamella (S_CL). We also compared the ordering variation of the rod blocks of triblock copolymers with that of rod-coil R_5C_4 diblock copolymers. The order parameter of the rod blocks for R_5C_4 copolymers is incorporated in Fig. 2e. It is obvious that the temperature at order-disorder transition (ODT) for R_5C_4 is higher than that of $R_5C_4R'_5$. In addition, the order parameter of R_5C_4 is relatively higher and increases more markedly with decreasing T. The results indicate that the ordering of the rod blocks is hindered by the chemically bonding constraint of another rod block to the diblock copolymer.

In the above, three critical points of $S = 0$ ($T = 3.7$), $S = 0.43$, and $S = 0.9$ were chosen. The first critical point of $S = 0$ ($T = 3.7$) corresponds to the Dis-to-IL phase transition, whereas the second critical point of $S = 0.43$ corresponds to the IL-to-NL phase transition. Due to the dramatic variation of the order parameter in the phase transition, both the Dis-to-IL and IL-to-NL phase transitions are considered to be first order [58]. Note that the critical point of $S = 0.43$ corresponds to point where the order parameter suddenly increases in the transition from isotropic lamella to nematic lamella (see Fig 2e). This critical value is consistent with that predicted by Maier-Saupe theory [59]. The critical value of $S = 0.9$, corresponding to the NL-to-S_CL phase transition, is chosen as the intersection points of two tangent lines to the curve (between $S \approx 0.43$ and $S \approx 1.0$) at the points near transitions. The NL-to-S_CL phase transition could be a second-order transition due to the continuous variation of the order parameters [58]. In what follows, these three critical points were approximately used to distinguish the phases.

Subsequently, we examined the effect of the length of coil blocks on the LC structures formed at a low temperature ($T = 1.0$). Three samples with $m = 3$, 4, and 5 were typically addressed, and the results are shown in Fig. 3a. These triblock copolymer systems all undergo a transition from isotropic structure to smectic C structure with decreasing the temperature. For $m = 3$ and 4, the structures are similar at $T = 1.0$, in which the rod blocks show similar inclination (see Fig. 3a1 and 3a2) tilting direction. However, for $m = 5$, there are two tilting directions for both **R** and **R'** blocks in the lamellar structure composed of alternating **R** and **R'** layers (see Fig. 3a3). The alternating appearance of two tilting directions in **R** or **R'** layers leads to the formation of arrowhead-like structure, as schematically shown in Fig. 3a3. This kind of complicated lamellar structure can be referred to as interdigitated-arrowhead lamellae that belong to the smectic C lamellae.

The interdigitated-arrowhead lamellar structure is an interesting finding of this work. Although both the **R** and **R'** blocks exhibit two different tilting directions with respect to the lamellar normal, the tilt angle are approximately the same. The structural symmetry of interdigitated-arrowhead lamellae can be contributed to the geometric symmetry of the copolymer architecture. As a matter of fact, the arrowhead-like lamellae with alternating appearance of rod alignments at two tilting directions have also been found in a rod-coil diblock copolymer system [30]. However, because of the only one kind of rod blocks, the alternating phenomenon of two kinds of rod layers is absent. Horsch et al. found that the rod-coil diblock copolymers with an aspect ratio of 5:1 of rod blocks can self-assemble into the arrowhead-like lamella at the fraction of $0.375 < f_c < 0.44$ of coil blocks, where f_c is relative ratio of coil bead number to total bead number [30]. The reason for the formation of arrowhead patterns between neighboring rod monolayers may be that the correlation between rod layers is weak due to the thick coil layers between them and the short range of the rod-rod interactions. The arrowhead morphology cannot be observed at a low f_c, and instead, the traditional smectic C structure

(a)

(a1)$R_5C_3R'_5$ **(a2)$R_5C_4R'_5$**

(a3)$R_5C_5R'_5$

(b)
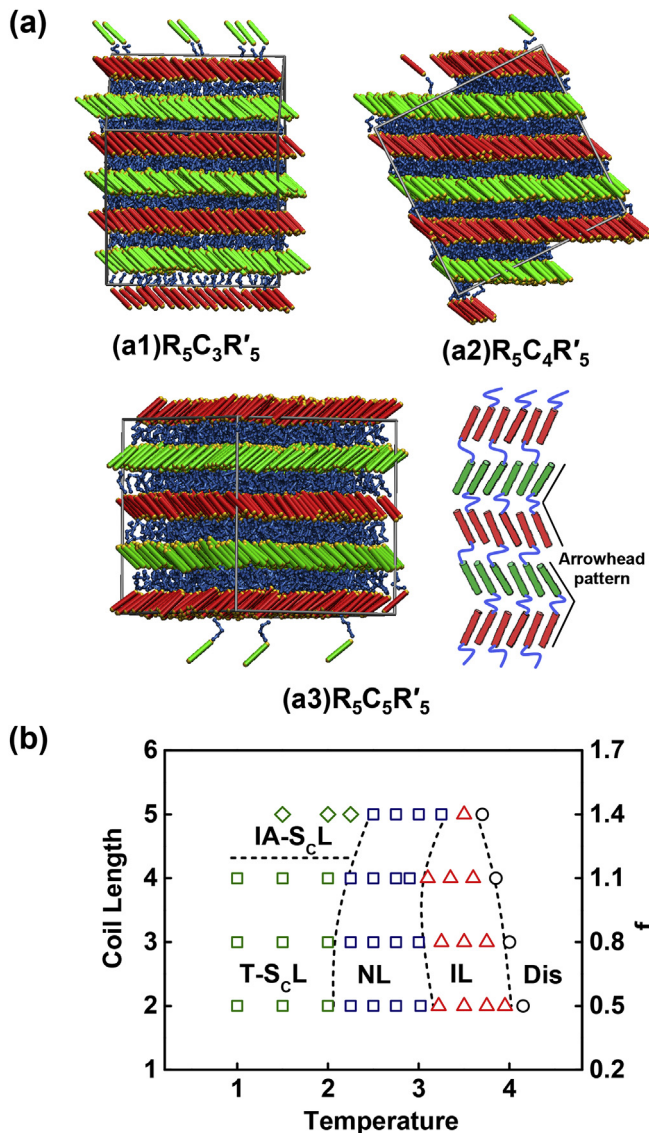
Fig. 3. (a) Snapshots of LC structures formed by symmetric $R_5C_mR'_5$ triblock copolymers with various lengths of coil blocks at a low temperature of $T = 1.0$: (a1) $m = 3$, (a2) $m = 4$, and (a3) $m = 5$. The sketch of the interdigitated-arrowhead lamella is also shown. (b) Stability regions of the structures formed by symmetric $R_5C_mR'_5$ triblock copolymers in the space of coil block length versus the temperature. The right axis shows the corresponding ratio f of coil length to rod length defined as $f = \frac{(n_{coil}-1)R_0+\sigma}{(n_{rod}-1)d+\sigma}$. Regions of disordered phase (Dis), isotropic lamella (IL), nematic lamella (NL), and smectic C lamella (S_CL) are shown. The smectic C lamella contains the traditional smectic C lamella (T-S_CL) and interdigitated-arrowhead lamella (IA-S_CL).

is formed, similar to our simulation. The block copolymers with shorter coil blocks can possess stronger attraction between the rod blocks due to the increased hydrophobicity of the copolymers or the increased attractive proportion (rod blocks) in the copolymers. This restricts the rod blocks to being packed along the same direction. In our study, the formation principle of interdigitated-arrowhead lamellae is similar to that of rod-coil diblock copolymers, but it is relatively more complicated due to the existence of two rod blocks.

Summarizing the results regarding the effects of the length of coil blocks and the temperature, the morphology stable regions of various LC structures were mapped out. The result is presented in Fig. 3b. To gain insight into the relative lengths of coil and rod blocks, the corresponding ratio of coil length to rod length was

given in the right axis. The morphologies observed include the disordered phase (Dis), isotropic lamella (IL), nematic lamella (NL), and smectic C lamella (S_CL), where the smectic C lamella contains the traditional smectic C lamella (T-S_CL) and interdigitated-arrowhead lamella (IA-S_CL). At higher temperature, the rod-coil-rod triblock copolymers are in a disordered state. The ODT happens with decreasing the temperature, and the isotropic lamella is formed. The ODT boundary shifts toward lower temperature with increasing the length of coil blocks. As the temperature further decreases, a transition from isotropic lamella to nematic lamella and then to smectic C lamella was shown. On the other hand, with increasing the length of coil blocks, the region of isotropic lamella becomes narrower, while the region widths of nematic lamella and smectic C lamella keep unchanged roughly. The boundary between nematic lamella and smectic C lamella tends to shift toward higher temperature, suggesting that at a constant T the smectic C lamella is easier to form than the nematic lamella for longer coil blocks. In addition, the interdigitated-arrowhead lamella is formed for longer coil blocks instead of the traditional smectic C lamella.

For the symmetric triblock copolymers, when we change the lengths of two rod blocks simultaneously, the LC structures of copolymers can also be changed. To demonstrate the effect of the length of rod blocks, we constructed the morphology stable regions of various LC structures in the space of the length of rod blocks versus the temperature, as shown in Fig. 4. The length of coil blocks was set as 4. It can be seen that the copolymers can form similar morphologies to those for various lengths of coil blocks. Obviously, the ODT boundary shifts toward lower temperature with decreasing the length of rod blocks. The order-order transition with the temperature has the same rule as above mentioned, that is, the transition from isotropic lamella to nematic lamella and then to smectic C lamella as the temperature decreases. With decreasing the length of rod blocks, the region of isotropic lamella becomes narrower, and the structure can only be observed for longer rod blocks. The boundary between nematic lamella and smectic C lamella tends to shift toward lower temperature, suggesting that at a constant T the smectic C lamella is easier to form than the nematic lamella for longer rod block. In addition, the interdigitated-arrowhead lamella is formed for the shorter rod block instead of the traditional smectic C lamella.

From Figs. 3b and 4, we learned that there are phase transitions from NL to T-S_CL (or IA-S_CL) with increasing the coil length or rod
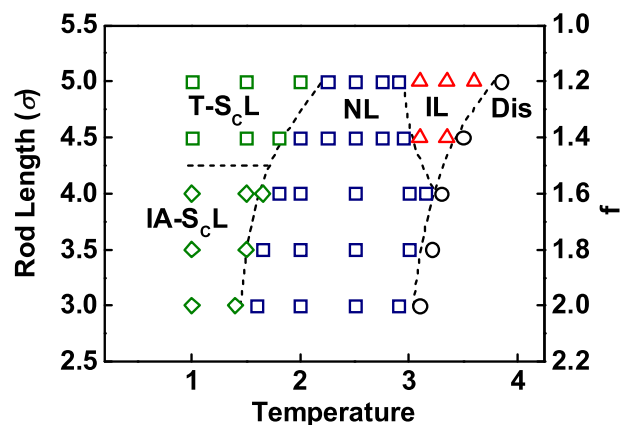
Fig. 4. Stability regions of the structures formed by symmetric $R_5C_4R'_5$ triblock copolymers in the space of rod block length versus the temperature. The right axis shows the corresponding ratio f of coil length to rod length. Regions of disordered phase (Dis), isotropic lamella (IL), nematic lamella (NL), and smectic C lamella (S_CL) are shown. The smectic C lamella contains the traditional smectic C lamella (T-S_CL) and interdigitated-arrowhead lamella (IA-S_CL).

length at certain temperatures. As the coil block is short, the rod blocks are randomly oriented to make the coil blocks relax and thus the NL is formed. However, the enthalpy would increase. As the coil block becomes long, the (long) rod blocks are well aligned to reduce the enthalpy without stretching the coil blocks too much. Therefore, the T-S$_C$L (or IA-S$_C$L) is formed. On the other hand, as the rod block is short, the attraction between rod blocks is smaller, and the entropy dominates the phase separation. As a result, the NL phase is favored. When the rod block is long, the attraction between rod blocks dominates the phase separation and the rod blocks tend to be well arranged in the structures. Under this condition, the T-S$_C$L (or IA-S$_C$L) with highly orientational rod blocks is preferred.

The dependencies of order parameters and tilt angles of two rod blocks on the temperature and lengths of coil blocks are shown in Fig. 5. From Fig. 5a—c, it can be seen that the S curves are almost overlapped for **R** and **R**′ blocks due to the length symmetry of triblock copolymer. We can also view the effect of the length of coil block. For $m = 3$ and 4, the S curves have two sharp rises which occur at $S \approx 0$ and $S \approx 0.43$, respectively. These correspond to two first-order Dis-to-IL and IL-to-NL phase transitions. For $m = 5$, however, the two sharp rises in the S curve are not obvious due to much narrower region of IL phases. The continuous variation of order parameters between $S \approx 0.43$ and $S \approx 1.0$ implies the NL-to-T-S$_C$L transition could be second order. In addition, the ODT temperature for $m = 5$ is slightly lower than those of $m = 3$ and 4. The difference in the order parameters may be ascribed to the structure diversity. Shorter length of coil blocks can decrease the freedom degree of rod blocks more greatly, decelerating the ordered packing of rod blocks. The tilt angle θ of rod blocks with respect to the interfacial normal, which is an important parameter characterizing whether the structures are smectic A or smectic C lamella, was calculated for the **R** and **R**′ blocks. The results are shown in Fig. 5d—f. In the low-temperature regions ($T < 2.0$), the tilt angles for all structures increase with decreasing the temperature, and have nearly overlapped curves for both the **R** and **R**′ blocks. In addition, the length of coil blocks was found to exert a less marked influence on the values of tilt angles.

Several theoretical reports on rod-coil block copolymers can provide evidences that the tilt angle of rod alignment increases with the decrease of temperature for rod-coil-rod triblock copolymers [25,26]. Matsen and Barrett used the SCFT in Semenov-Vasilenko model to examine the phase behavior of rod-coil diblock copolymers [25]. It was found that at certain contents of coil blocks, the LC structures can be transformed from smectic A to smectic C phases with increasing the interaction parameter χN. It implies that stronger interactions can lead to a more tilted packing of rod blocks. In our system of rod-coil-rod triblock copolymers, the two rod blocks are more inclined at a lower temperature. The decrease of temperature can correspond to the increase in χN, and the increase in the tilt angles represents a more tilted alignment of rod blocks in the lamellar structures. The variation tendency for tilt angles of two blocks in the triblock copolymers is in accordance with the theoretical predictions of rod-coil diblock copolymers.

3.2. Hierarchical LC structures self-assembled from asymmetric triblock copolymers

In this subsection, we focused on the self-assembled structures of asymmetric triblock copolymers. The models of **R**$_5$**C**$_5$**R**′$_5$ copolymers with various **R**′ block lengths were built, and four typical samples of $L' = 3.0\sigma$, $L' = 3.5\sigma$, $L' = 4.0\sigma$, and $L' = 4.5\sigma$ were considered. We also examined the self-assembled structures of the **R**$_5$**C**$_m$**R**′$_5$ copolymers with a fixed L' (=3.5σ) as the length of coil blocks m is variable. These systems were cooled slowly down from a high temperature for a long enough time. By combining the effects of the temperature and the length of **R**′ blocks ($m = 5$) or the length of **C** blocks ($L' = 3.5\sigma$), the morphology stability regions were mapped out. Finally, the order parameters and tilt angles of two rod blocks were characterized.

Fig. 6 shows the typical results of the LC structures formed at various temperatures and various lengths of **R**′ blocks. The temperature dependence of morphologies for $L' = 3.5\sigma$ is presented in Fig. 6a. When the temperature is very high ($T = 5.5$), the copolymers first exhibit an isotropic phase. By cooling the system, the isotropic lamella structure is formed at $T = 4.25$, in which the packing ordering of both the two kinds of rod blocks are very low. As the temperature decreases to 3.5, the rod blocks show moderate ordering, and a kind of hierarchical lamellar structure appears with
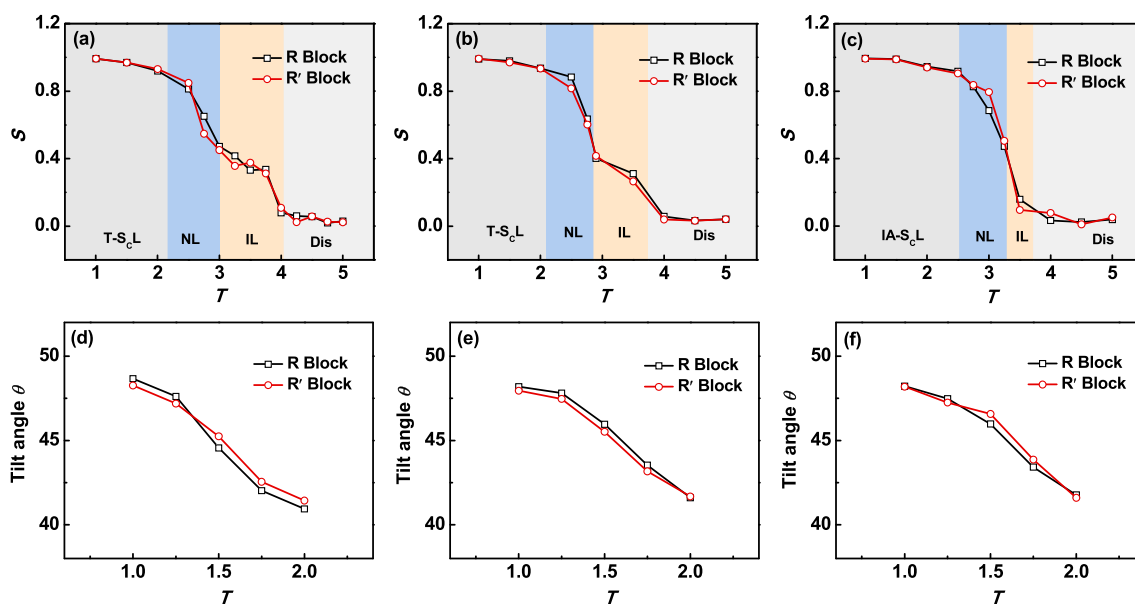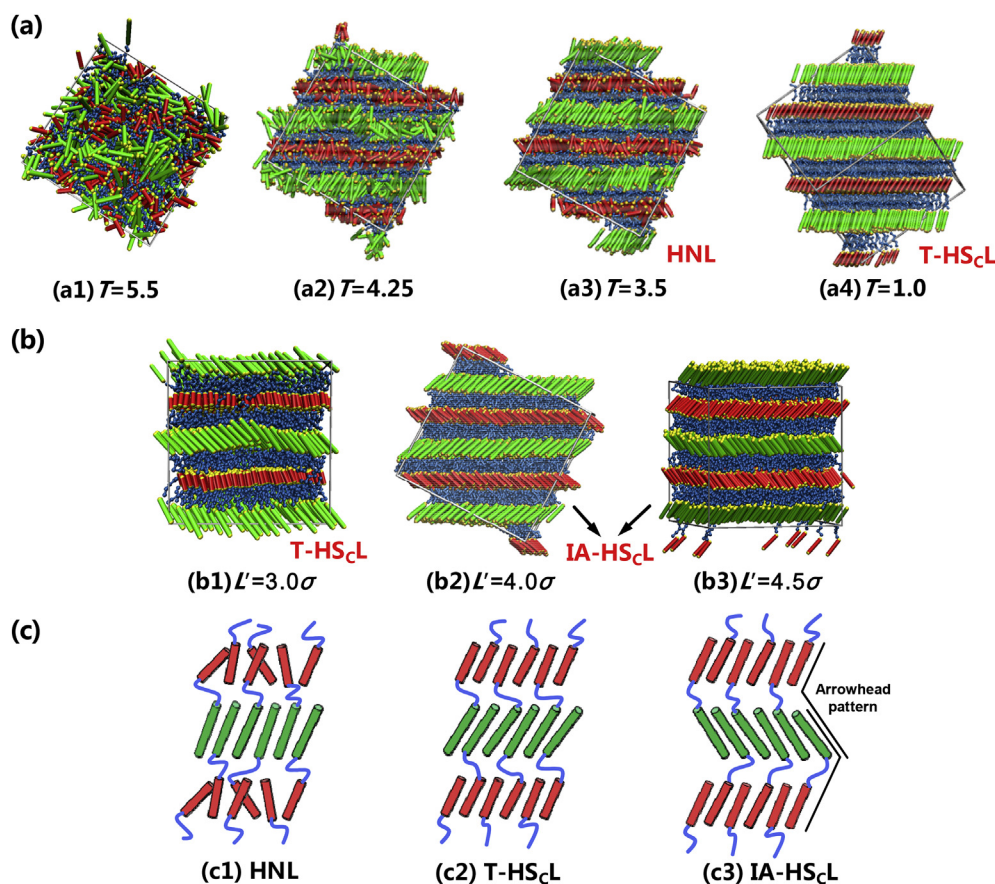

Fig. 5. (a—c) Order parameters S and (d—f) tilt angles θ of **R** and **R**′ blocks in the LC structures formed by symmetric **R**$_5$**C**$_m$**R**′$_5$ triblock copolymers as functions of the temperature. The m values are (a, d) $m = 3$, (b, e) $m = 4$, and (c, f) $m = 5$.
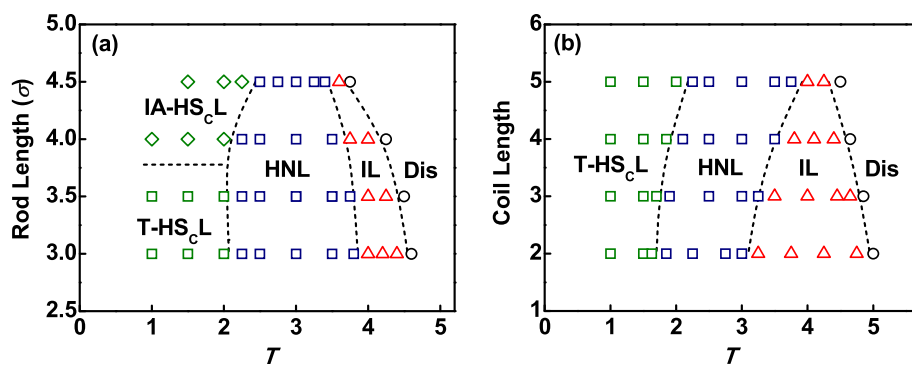
Fig. 6. (a) Snapshots of LC structures formed by asymmetric $\mathbf{R}_5\mathbf{C}_5\mathbf{R}'_5$ triblock copolymers with $L' = 3.5\sigma$ at various temperatures: (a1) $T = 5.5$, (a2) $T = 4.25$, (a3) $T = 3.5$, and (a4) $T = 1.0$. (b) Snapshots of LC structures for various rod block lengths at a low temperature of $T = 1.0$: (b1) $L' = 3.0\sigma$, (b2) $L' = 4.0\sigma$, and (b3) $L' = 4.5\sigma$. The hierarchical LC structures have been marked. (c) Schematic representation of the hierarchical LC structures: (c1) HNL, (c2) T-HS$_C$L, and (c3) IA-HS$_C$L.

two LC phases at different length scales due to different lengths of two kinds of rod blocks. Moreover, the ordering degrees of the **R** and **R'** blocks are discrepant, where the longer **R** blocks possess higher packing ordering than the shorter **R'** blocks. We defined this structure as hierarchical nematic lamella (HNL). With further decreasing the temperature, the copolymers form the hierarchical smectic C lamella (HS$_C$L), in which both the **R** and **R'** blocks exhibit highly ordered arrangement. Fig. 6b shows the hierarchical smectic C lamellar structures at $T = 1.0$ for various lengths of **R'** blocks. As shown in the figure, the tilting directions of **R** and **R'** blocks can be changed by tuning the length of **R'** blocks (L'). When L' increases from 3.0σ to 4.0σ, the traditional smectic C (T-HS$_C$L) structure is transformed into the arrowhead-like smectic C (IA-HS$_C$L) structure (Fig. 6b1-b2). In this structure, the tilting directions of the **R** and **R'** blocks are different, although each kind of **R** blocks (or **R'** blocks) is inclined toward one direction. With increasing the L' to 4.5σ, the interdigitated-arrowhead lamella was observed similar to the structure formed by the symmetric copolymers (see Fig. 3a4), in which both the **R** and **R'** blocks tilt along two different directions. These arrowhead-like structures are all in the scope of smectic C structures. In addition, to distinguish different hierarchical LC structures, the sketches for these typical structures are presented in Fig. 6c, in which the structure details and chain distributions are clearly shown.

The morphology stable regions of various LC structures in the space of the temperature versus the length of **R'** blocks or in the space of the temperature versus the length of **C** blocks were presented in Fig. 7a–b. The regions of disordered phase (Dis), isotropic

lamella (IL), hierarchical nematic lamella (HNL), and hierarchical smectic C lamella (HS$_C$L) are shown, where the HS$_C$L contains the traditional smectic C lamella (T-HS$_C$L) and interdigitated-arrowhead lamella (IA-HS$_C$L). The asymmetric triblock copolymer with two kinds of rod blocks of different lengths was proved to be a promising model for creating hierarchical LC structures. The phase regions indicate a transition from Dis to IL, then to HNL, and finally to HS$_C$L as the temperature decreases. As shown in Fig. 7a, when the length of rod blocks L' increases ($m = 5$), the regions of IL and HNL become narrow. The boundary between HNL and HS$_C$L shifts towards higher temperature, whereas the ODT boundary and the boundary between IL and HNL shift to lower temperature. The copolymers tend to form the interdigitated-arrowhead smectic C lamellae for longer **R'** blocks but to form traditional smectic C lamellae for shorter **R'** blocks at low temperature. Fig. 7b shows the morphology stable regions for asymmetric copolymers with various lengths of coil blocks at $L' = 3.5\sigma$. For the selected range of coil block length (2–5), the interdigitated-arrowhead lamellae cannot be obtained, which is controlled by the relative length ratio of the rod and coil blocks. When the length of coil blocks is long, the IA-HS$_C$L structure is easy to form. At $m = 5$, the T-HS$_C$L structure is formed, and therefore a decrease of m goes against the formation of the IA-HS$_C$L structure. In addition, we can also view the relationship between phase boundary and the length of coil blocks. As the length of coil block increases, both the boundaries between HNL and HS$_C$L and between IL and HNL move to higher temperature, but the ODT boundary shifts to lower temperature.

In order to understand the structure diversity among these

Fig. 7. Stability regions of the structures formed by asymmetric $R_5C_mR'_5$ triblock copolymers (a) in the space of R' rod block length versus the temperature at $m = 5$ and (b) in the space of C block length versus the temperature at $L' = 3.5\sigma$.

hierarchical LC structures, the order parameters and tilt angles of the R and R' blocks in the LC structures formed by asymmetric $R_5C_5R'_5$ triblock copolymers were calculated at various lengths of R' blocks. The results are given in Fig. 8. As shown in Fig. 8a–c, at moderate temperatures, the order parameter of the R blocks is higher than that of the R' blocks. This difference becomes more marked as the R' blocks are short. That is because the R block is longer than the R' block. The large difference between the orderings of the R and R' blocks leads to the structural hierarchy of the nematic lamellae. Note that although the order parameters are different for the R and R' blocks, the critical points ($S \approx 0$, 0.43, and 0.9) for the phase transitions are almost the same. On the other hand, the tilt angles of R and R' blocks are also different, as shown in Fig. 7d–f. The longer R blocks possess larger tilt angles relative to shorter R' blocks. The divergence in the tilt angles of the R and R' blocks becomes weak with increasing the architectural symmetry of the copolymers (increase in L'). It was also found that the length of rod block has a pronounced influence on the values of tilt angles, in contrast to the length of coil blocks. The increase in L' can elevate the tilt angles of both the R and R' blocks. It can be noted from Fig. 8a–c that the length of R' blocks can affect the ODT

temperature significantly. The ODT temperature decreases with increasing the length of R' blocks.

In this work, we discovered the hierarchical LC structures in the self-assembly systems of rod-coil-rod triblock copolymers. In recent experimental studies, the hierarchical LC structures have been prepared by block copolymers comprised of two kinds of rigid blocks. For example, Iatrou et al. studied the self-assembly of PBLG-*b*-PLP where the PBLG and PLP are rod blocks with helical structures. It was found that these copolypeptides can form hierarchical LC fibles. In fibers, the PBLG helices are preferentially oriented along the fiber axis, whereas the PLP helices were found to be unoriented [20]. Haataja et al. observed the double smectic structures with alternating PBLG and PLL(diC4P) smectic layers with perpendicular alignment in the PBLG-*b*-PLL complexed by diC4P [22]. In these structures, the different kinds of rod blocks exhibit different LC states in the domains. We also observed various hierarchical LC structures such as HNL where two kinds of rod blocks show different LC states or different orientations in the same LC states. The structural feature between the experiment and the simulation are essentially identical. In particular, Iatrou et al. reported zig-zag lamellar structures formed by the PBLG-*b*-PBLHyP
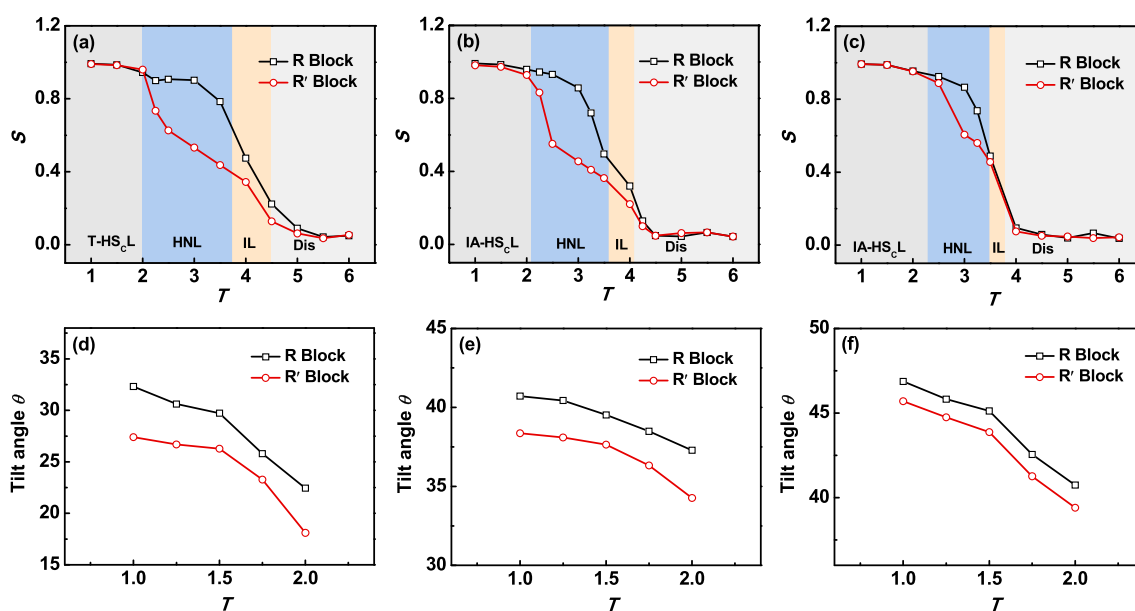
Fig. 8. (a–c) Order parameters S of R and R' blocks in the LC structures formed by asymmetric $R_5C_5R'_5$ triblock copolymers as functions of the temperature at various lengths of R' blocks: (a) $L' = 3.5\sigma$, (b) $L' = 4.0\sigma$, and (c) $L' = 4.5\sigma$. (d–f) Tilt angles θ of R and R' blocks as functions of the temperature at various lengths of R' blocks: (d) $L' = 3.5\sigma$, (e) $L' = 4.0\sigma$, and (f) $L' = 4.5\sigma$.

copolymers, where the PBLHyP tilt to match the PBLG periodicity [21]. The formation of zig-zag lamellar structures is due to the mismatch in the packing periodicities of the PBLG and PBLHyP helices. These structures are similar to the IA-HS$_C$L where the two kinds of rod blocks are respectively inclined to form interdigitated-arrowhead structures (see Fig. 6c3). We also found that the formation of the IA-HS$_C$L is due to the mismatch of the lengths of two kinds of rod blocks.

The architectural asymmetry of rod-coil-rod triblock copolymers was found not only to determine the morphologies of formed LC structures, but also to influence the order-disorder transition and order-order transition. The hierarchical nematic and smectic structures are interesting findings of this work. In the nematic structures, two kinds of rod blocks possess different packing orderings. In the smectic structures, although the orderings of two kinds of rod blocks are essentially the same, they show different tilting directions and tilt angles. This leads to the formation of interdigitated-arrowhead lamellae. The results can deepen our understanding of the formation of hierarchical LC structures. The hierarchical LC structures could have both the orientational ordering properties of the LC systems and rubber elasticity of polymer domains, similar to the internal structure of LC elastomers [60,61]. Since the LC phases can response to the change of temperature due to the disorder-order transition or order-order transition, the LC phases at two length scales in the hierarchical LC structures may lead to dual hierarchical responses. The dual-stimuli-response materials with such hierarchical LC structures could be used as human-made muscle-like materials [62], which could exhibit advantages over traditional LC elastomers. In addition, they can find their potential applications in fields of optoelectronic devices, high-modulus fibers, and biosystems.

4. Conclusions

We applied Brownian dynamics simulations to investigate the self-assembly behavior of rod-coil-rod triblock copolymers. The morphologies of LC structures were found to be dependent of the temperature, the symmetry of copolymer architecture, and the length of blocks. For the symmetric block copolymers, with decreasing the temperature, the morphology is transformed from isotropic lamella to nematic lamella, and then to smectic C lamella. The morphology regions of various LC structures in space of the temperature versus the length of blocks were obtained. In these LC structures, the order parameter and tilt angle of the **R** and **R**′ blocks are nearly the same. For the asymmetric block copolymers, the **R** and **R**′ blocks of different lengths were found to exhibit different ordering degrees and tilt angles in the structures. The asymmetric design of copolymer architectures leads to the formation of various hierarchical LC structures, including hierarchical nematic lamella and hierarchical smectic C lamella. The lengths of blocks and the temperature show a pronounced influence on the morphologies of the hierarchical LC structures and the orientation of the rod blocks. The present work provides a promising route toward constructing hierarchical liquid crystalline structures.

Acknowledgements

References

[1] K.K. Tenneti, X. Chen, C. Li, Y. Tu, X. Wan, Q. Zhou, I. Sics, B.S. Hsiao, J. Am. Chem. Soc. 127 (2005) 15481.
[2] X. Chen, Z. Shen, X. Wan, X. Fan, E. Chen, Y. Ma, Q. Zhou, Chem. Soc. Rev. 39 (2010) 3072.
[3] C.J. Tschierske, Mater. Chem. 11 (2001) 2647.
[4] K.K. Tenneti, X. Chen, C. Li, Z. Shen, X. Wan, X. Fan, Q. Zhou, L.X. Rong, B.S. Hsiao, Macromolecules 42 (2009) 3510.
[5] J.T. Chen, E.L. Thomas, C.K. Ober, G. Mao, Science 273 (1996) 343.
[6] E.L. Thomas, J.T. Chen, M.J.E. O'Rourke, C.K. Ober, G. Mao, Macromol. Symp. 117 (1997) 241.
[7] M. Lee, B.K. Cho, W.C. Zin, Chem. Rev. 101 (2001) 3869.
[8] X. Zhu, L. Wang, J. Lin, J. Phys. Chem. B 117 (2013) 5748.
[9] D.G. Dervichian, Mol. Cryst. Liq. Cryst. 40 (1997) 19.
[10] I.W. Hamley, Introduction to Soft Matter: Polymers, Colloids, Amphiphiles and Liquid Crystals, John Wiley & Sons Ltd, Chichester, UK, 2000.
[11] S. Junnila, N. Houbenov, S. Hanski, H. Iatrou, A. Hirao, N. Hadjichristidis, O. Ikkala, Macromolecules 43 (2010) 9071.
[12] S. Valkama, H. Kosonen, J. Ruokolainen, T. Haatainen, M. Torkkeli, R. Serimaa, G. ten Brinke, O. Ikkala, Nat. Mater. 3 (2004) 872.
[13] T. Ruotsalainen, J. Turku, P. Heikkilä, J. Ruokolainen, A. Nykänen, T. Laitinen, M. Torkkeli, R. Serimaa, G. ten Brinke, A. Harlin, Adv. Mater. 17 (2005) 1048.
[14] Y. Matsushita, Macromolecules 40 (2007) 771.
[15] J. Masuda, A. Takano, J. Suzuki, Y. Nagata, A. Noro, K. Hayashida, Y. Matsushita, Macromolecules 40 (2007) 4023.
[16] W. Li, F. Qiu, A. Shi, Macromolecules 45 (2012) 503.
[17] W. Li, A. Shi, Macromolecules 42 (2009) 811.
[18] Y. Xu, W. Li, F. Qiu, Y. Yang, A. Shi, Phys. Chem. Chem. Phys. 13 (2011) 12421.
[19] J. Ruokolainen, G. ten Brinke, O. Ikkala, Adv. Mater. 11 (1999) 777.
[20] R. Graf, H.W. Spiess, G. Floudas, H.-J. Butt, M. Gkikas, H. Iatrou, Macromolecules 45 (2012) 9326.
[21] M. Gkikas, J.S. Haataja, J. Seitsonen, J. Ruokolainen, O. Ikkala, H. Iatrou, N. Houbenov, Biomacromolecules 15 (2014) 3923.
[22] J.S. Haataja, N. Houbenov, H. Iatrou, N. Hadjichristidis, A. Karatzas, C.F.J. Faul, P. Rannou, O. Ikkala, Biomacromolecules 13 (2012) 3572.
[23] R. Maeda, T. Hayakawa, M. Tokita, R. Kikuchi, J. Kouki, M. Kakimoto, H. Urushibata, React. Funct. Polym. 69 (2009) 519.
[24] H. Xie, C. Jie, Z. Yu, X. Liu, H. Zhang, Z. Shen, E. Chen, Q. Zhou, J. Am. Chem. Soc. 132 (2010) 8071.
[25] M.W. Matsen, C. Barrett, J. Chem. Phys. 109 (1998) 4108.
[26] V. Pryamitsyn, V. Ganesan, J. Chem. Phys. 120 (2004) 5824.
[27] J. Chen, C. Zhang, Z. Sun, Y. Zheng, L. An, J. Chem. Phys. 124 (2004) 104907.
[28] Y. Xia, J. Chen, Z. Sun, T. Shi, L. An, Y. Jia, J. Chem. Phys. 131 (2009) 144905.
[29] M.A. Horsch, Z. Zhang, S.C. Glotzer, Phys. Rev. Lett. (2005) 95, 056105.
[30] M.A. Horsch, Z. Zhang, S.C. Glotzer, Soft Matter 6 (2010) 945.
[31] M.A. Horsch, Z. Zhang, S.C. Glotzer, J. Chem. Phys. 125 (2006) 18490.
[32] A. AlSunaidi, W.K. den Otter, J.H.R. Clarke, Philos. Trans. R. Soc. Lond. A 362 (2004) 1773.
[33] A. AlSunaidi, W.K. den Otter, J.H.R. Clarke, J. Chem. Phys. 130 (2009) 124910.
[34] A. Halperin, Europhys. Lett. 10 (1989) 549.
[35] A.N. Semenov, S.V. Vasilenko, Zh Eksp. Teor. Fiz. 90 (1986) 124.
[36] D.R.M. Williams, G.H. Fredrickson, Macromolecules 25 (1992) 3561.
[37] J. Lin, S. Lin, L. Zhang, T. Nose, J. Chem. Phys. (2009) 130, 094907.
[38] K. Xu, R. Guo, B. Dong, L. Yan, Soft Matter 8 (2012) 9581.
[39] Z. Liu, R. Guo, G. Xu, Z. Huang, L. Yan, Nano Lett. 14 (2014) 6910.
[40] R. Guo, Z. Liu, X. Xie, L. Yan, J. Phys. Chem. Lett. 4 (2013) 1221.
[41] J. Huang, Z. Fan, Z. Ma, J. Chem. Phys. (2013) 139, 064905.
[42] A.K. Omar, B. Hanson, R.T. Haws, Z. Hu, D.A.V. Bout, P.J. Rossky, V. Ganesan, J. Phys. Chem. B 119 (2015) 330.
[43] Z. Ma, J. Huang, M. Luo, Soft Matter 11 (2015) 4932.
[44] Y. Zhou, S. Song, X. Long, C. Zhang, Y. Chen, Macromol. Theory Simul. 23 (2014) 490.
[45] J. Chen, Z. Sun, C. Zhang, L. An, Z. Tong, J. Chem. Phys. (2008) 128, 074904.
[46] S. Lin, N. Numasawa, T. Nose, J. Lin, Macromolecules 40 (2007) 1684.
[47] S. Lin, X. He, Y. Li, J. Lin, T. Nose, J. Phys. Chem. B 113 (2009) 13926.
[48] Y. Li, S. Lin, X. He, J. Lin, T. Jiang, J. Chem. Phys. (2011) 135, 014102.
[49] Z. Zhang, M.A. Horsch, M.H. Lamm, S.C. Glotzer, Nano Lett. 3 (2003) 1341.
[50] K. Kremer, G.S. Grest, J. Chem. Phys. 92 (1990) 5057.
[51] G.S. Grest, K. Kremer, T.A. Witten, Macromolecules 20 (1987) 1376.
[52] C.R. Iacovella, S.C. Glotzer, Nano Lett. 9 (2009) 1206.
[53] C.L. Phillips, C.R. Iacovella, S.C. Glotzer, Soft Matter 6 (2010) 1693.
[54] G.S. Grest, K. Kremer, Phys. Rev. A 33 (1986) 3628.
[55] G.S. Grest, M.D. Lacasse, J. Chem. Phys. 105 (1996) 10583.
[56] M.P. Allen, D.J. Tildesley, Computer Simulations of Liquids, Oxford University Press, New York, 1987.
[57] S. Plimpton, J. Comput. Phys. 117 (1995) 1.
[58] S.J. Blundell, K.M. Blundell, Concepts in Thermal Physics, Oxford University Press, New York, 2008.
[59] W. Maier, A.Z. Saupe, Naturforsch A 13 (1958) 564 (in German).
[60] M.-H. Li, P. Keller, J. Yang, P.-A. Albouy, Adv. Mater. 16 (2004) 1922.
[61] M.-H. Li, P. Keller, Philos. Trans. R. Soc. A 364 (2006) 2763.
[62] P.G. de Gennes, M. Hébert, R. Kant, Macromol. Symp. 113 (1997) 39.